Assessment of Deformation Twinning in Cold Rolled Austenitic Stainless Steels with Electron Back Scatter Diffraction

I. I. Ahmed[1*], D. Wright[1], J. A. Adebisi[2], I. N. Aremu[2], T. Yahaya[2] and J. Quita da Fonseca[1]

[1]Material Performance Centre, University of Manchester, Oxford Road, Manchester, M13 9PL, UK.
[2]Department of Materials and Metallurgical Engineering, University of Ilorin, Ilorin, Nigeria.

ABSTRACT: Deformation twinning has traditionally been studied with Transmission Electron Microscopy (TEM). In this study, an assessment of deformation twinning in Austenitic Stainless Steel (ASS), type 304L, cold rolled to 20% reduction was investigated using Scanning Electron Microscopy (SEM) and Electron Back Scatter Diffraction (EBSD) techniques rather than the conventional TEM. The study revealed the presence of deformation twins in the cold rolled grains of ASS. It emerged from the study that the deformation twins observed may facilitate localised heterogeneous deformation and development of internal stresses within the grain.

KEYWORDS: Cold rolled; Twinning; Deformation; Dislocation; SEM; EBSD

[Received April 1 2014; Revised May 28 2014; Accepted June 9 2014]

I. INTRODUCTION

The performance of Austenitic Stainless Steels (ASS) is considered satisfactory due to their good combination of high strength, ductility and general corrosion resistance even at elevated temperature (Couvant et al., 2005, Garda, 2000, Garcia et al., 2000). They are widely used in process plants, cryogenic plants, food industry and nuclear industry including high temperature water conditions in pressurised water reactor and boiling water reactor environments (Arioka et al., 2007).

Austenitic Stainless Steels are cold worked through plastic deformation at ambient temperature. The performance of material can be influenced by the type and amount of previous plastic deformation (Hagiwara et al., 2001, Ahmed et al., 2013). Some of the reasons why cold work may be carried out include: enhancement of surface properties during manufacturing and after fabrication processes, through-thickness reduction and strengthening purposes (Kain et al., 2004, Fu et al., 2009). During cold working, strength of material and hardness increase significantly at the expense of ductility due to increasing dislocation density and twin bands (Callister, 2003, Lozano-Perez et al., 2009, Murugesan et al., 2012, Ahmed et al., 2013). The increase in Stress Corrosion Cracking (SCC) susceptibility of cold worked ASS has been identified with factors which include: higher yield strength of cold worked material and plastic strain field gradient ahead of crack (Arioka et al., 2007, Andresen et al., 2005, Busby and Was, 2005), localised heterogeneous deformation of cold worked microstructures including strain induced martensite, retained delta ferrite and twin bands in austenite matrix (Spencer et al., 2009, Enami, 2005, ASM Handbook, 2000).

Austenitic Stainless Steels belong to group of material which have low to moderate stacking fault energy and propensity to develop stacking faults, deformation twins, and planar dislocation structures. The predominant deformation mechanism in ASS is by slip. However, the lower stacking fault energy of Austenitic Steels makes the formation of deformation twins favourable (Lee et al., 2007, Scheriau et al., 2011, Tsakiris and Edmonds, 1999). The effects of slip and twinning on deformation mechanism of polycrystalline materials have gained considerable attention in recent time and, the significance of twinning is becoming increasingly apparent. One particular area of relevance is the crystal plasticity models which have been used in prediction of macroscopic flow stress. However, the model has not been quite successful in other important areas including the prediction of Bauschinger effect because of its inability to incorporate the significant effect of twinning and precipitates (Karaman et al., 2002).

Deformation twinning has traditionally been studied with Transmission Electron Microscopy (TEM), in this study, an assessment of deformation twinning in cold rolled ASS, type 304L was carried out using SEM and EBSD techniques. The aim was to show the SEM and EBSD capability of assessing deformation twins after cold rolling and to gain a better understanding of the possible roles of deformation twinning in the localised heterogeneous deformation of ASS.

II. MATERIALS AND EXPERIMENTAL PROCEDURES

A. Material

The material used for this study was low carbon grade ASS, Type 304L, with the chemical composition shown in Table 1. The ASS plate (300 × 100 × 30 mm) as-received was initially solution annealed at 1050°C for 30 minutes and quenched in water. Fast cooling was done to prevent probable

* Corresponding author's email address: Ismaila.ahmed@yahoo.com

intergranular precipitation of the chromium carbide by sensitisation process (Garcia et al., 2002). The material was subsequently heat treated at 400°C and furnace cooled to partially relieve internal stresses and remove any martensite which might have formed due to fast cooling. Preliminary tests carried out on the annealed sample showed that the average grain size and 0.2% offset yield strength of the annealed material were 68 μm and 280 MPa respectively. The material was subsequently cold worked by uniaxial rolling.

Table 1: Chemical composition of as-received ASS Type 304L (wt %).

C	Cr	Mn	N	Ni	P	S	Si
0.030	18.387	1.804	0.086	8.133	0.034	0.005	0.411

B. Cold Rolling

Cold working could be achieved through a number of methods. However, cold rolling was used because it is easier to achieve different degrees of cold work through reduction in the sample thickness and it equally allows test samples to be manufactured from different orientations of the rolled plates. Annealed material was cold worked by multipass uniaxial rolling to 20% reductions in thickness. Each rolling pass corresponds to thickness reduction of 0.5 mm and the final thickness of rolled plates reduced from 30 mm to 27 mm. The degree of cold work was determined using eqn. (1) (Dieter and Bacon, 1986). Schematic illustration of the rolling process is shown in Figure 1. Sample for SEM was extracted from the centre of the rolled plate to ensure the test sample was homogeneous. The test sample was sectioned from Normal-Rolling (N-R) orientation of the cold rolled sample.

$$Work\ \text{Cold}\ (\%) = \frac{h_o - h_f}{h_o} \quad (1)$$

Where h_o and h_f are the initial and final through thickness dimensions respectively.

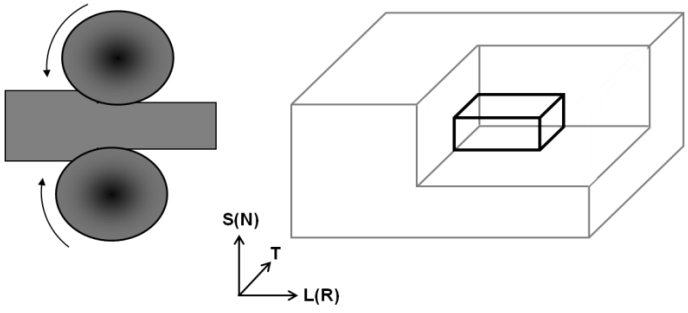

Figure 1: Schematic Diagram of Cold Rolling Process and Sample Orientations in Rolled Plate.

C. Scanning Electron Microscopy and Electron Back Scatter Diffraction

The dimensions of sample used for SEM and EBSD were 10 × 10 × 10 mm. The sample was extracted from the centre of cold rolled plate (see Figure 1) away from the highly deformed outer skin. The sample preparation included wet grinding with increasingly fine silicon carbide paper in order of 400, 600, 800, 1200 and 2500 grit sizes. The sample was subsequently polished with a diamond pastes containing 6 μm and 1μm particle sizes. The sample was further polished using Oxide Polishing Suspension (OPS) containing colloidal silica, with typical particle size of 0.05 μm for 30 minute. This was necessary to remove polishing scratches and to ensure strain-free surface for EBSD technique. EBSD allowed crystallographic information to be obtained inside the SEM from small volumes, which is comparatively larger and more representative of the material than TEM sample.

The EBSD maps were formed by focussed electrons probe scanning from point to point across a grid of positions on the bulk sample surface inside SEM chamber. At each point, electrons are diffracted from the lattice planes of crystal at the Bragg's angle, 2θ. Some of the electrons backscattered from the sample were collected by detector which comprised of scintillator screen coupled by lens to a photon sensitive imaging detector called Charge Coupled Device (CCD) camera, to form EBSD pattern. The SEM stage with the sample was tilted to 70^{o}C towards the detector to increase the quality of the pattern obtained (see Figure 2). Each pattern contained many Kikuchi bands, which appeared at first glance to have a parallel straight edge, but actually was curved at edges, consequent of hyperbola formed by the intersection of Kossel diffraction cones with detector plane. The patterns were then transferred from CCD camera to the computer for indexing with the standard materials from the database and for determination of crystal orientation (Wilkinson and Britton, 2012, Randle and Engler, 2000).

An in-built Hough algorithm was then used to convert the nearly straight bands from lines to points which are easily located. With the knowledge of experimental geometry, the peak locations were converted to a table of interplanar angles and compared with look up tables of expected angles for the phases present within the sample. Hence, a detailed mapping of the sample crystallography including crystal type, crystal orientation and pattern quality were obtained. The Field Emission Gun Scanning Electron Microscope (FEGSEM) used for imaging was installed with Hikari EBSD detector for data acquisition.

Secondary electron and back scatter electrons were used for SEM imaging and orientation contrast respectively at accelerating voltage of 20 kV. Data were acquired at step sizes of 0.5 μm. The samples were indexed as Face-Centred Cubic (FCC) and Body-Centred Cubic (BCC) Iron. The acquired EBSD data were analysed and processed into inverse pole figure map with EDAX OIM™ Analysis software.

III. RESULTS AND DISCUSSION

The result of scanning electron microscopy carried out on 20% cold rolled sample is shown in Figure 3. The SEM micrograph showed what appeared to be predominantly slip bands with little mean of identifying the deformation twins

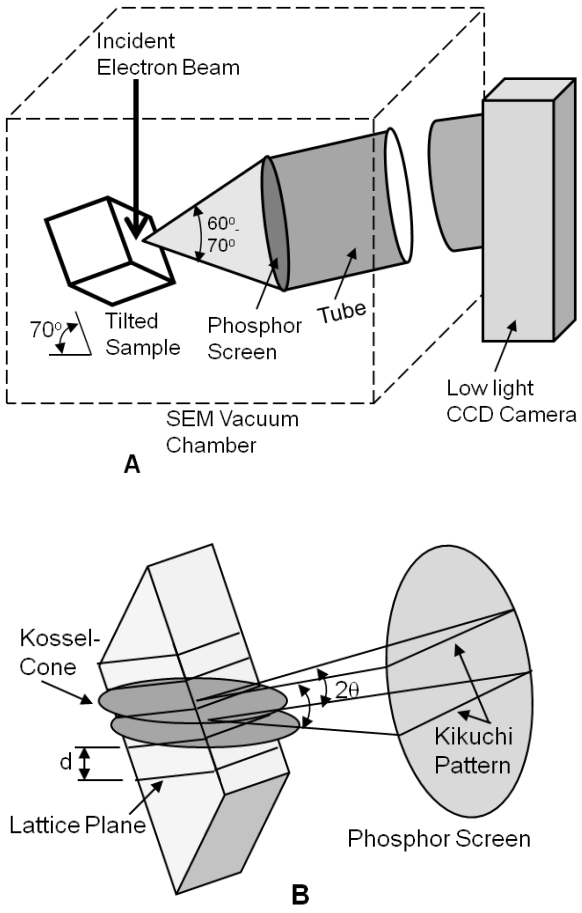

Figure 2: Schematic Diagram of EBSD Set-up (A) and Projection of Kikuchi Lines from a Crystal in Tilted Sample (B).

present (Figures 3A). The EBSD image quality and inverse pole figure maps revealed the deformation twins which are delineated in gold colour (see arrows) in Figures 3B and 2C respectively. The orientation contrast map of the grains is shown in Figure 3D, showing the deformation twins in greater details within the grains. In slip deformation mechanism, the movement of atoms occurred over a whole atomic distance without change in the orientation or structure of the lattice. However, twinning causes the movement of atom to occur over a fraction of inter-atomic distance thus resulting in lattice distortion (Elgun, 1999). Consequently, twin boundaries act as an impediment which may limit the mean free path of dislocations (Karaman et al., 2002, Jimenez and Frommeyer, 2010). The synergistic effects of both lattice distortion and impediment of the twin boundaries to the dislocation motion may be responsible for strain hardening and increase in strength of the cold rolled material.

The results of TEM study on deformation twinning carried out by (Karaman et al., 2002) are shown in Figure 2. The TEM micrographs indicate twin and microstructural features in ASS 316L, subjected to 15%, 10% and 24% tensile strain along [111], [001] and [011] directions respectively. The evidence of twinning and interaction of dislocations with the twin boundaries shown in the TEM micrographs is consistent with results elsewhere (Lee et al., 2007, Fu et al., 2009). This

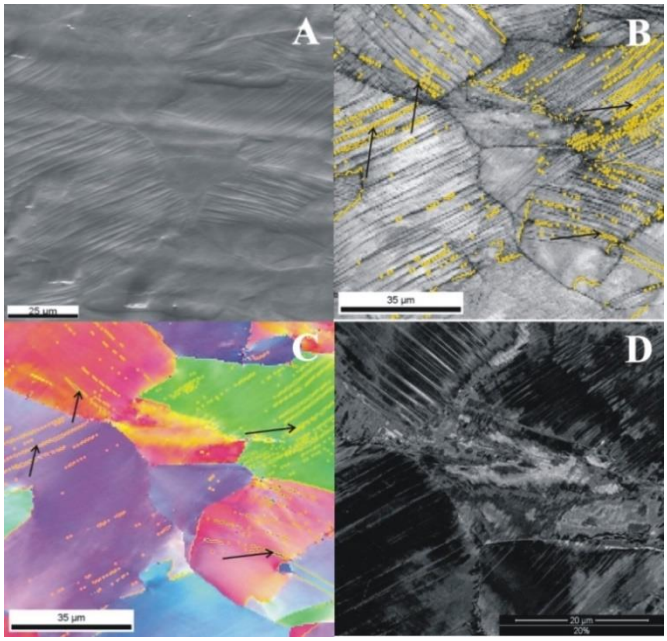

Figure 3: SEM Micrographs of 20% Cold Rolled ASS, Type 304L: Forward Scatter Electron Micrograph (A) and EBSD Micrographs Showing: Image Quality Map with Twin Boundaries (indicated with arrows) (B), Inverse Pole Figure Map with Twin Boundaries (C), and Orientation Contrast (D).

phenomenon underpins the explanation for increased strength due to strain hardening of cold worked materials. However, saturation of twinning and the formation of cell substructures within the twin lamellae (see Figure 2A) are likely to cause a decrease in the strain hardening of the region due to dislocation annihilation. The existence of layers of strong and weak regions can lead to heterogeneous deformation and residual stresses at a localised scale within the grain. This may equally provide easy propagation route for transgranular stress corrosion cracking in heavily cold worked material. The relatively lower amount of twins and the evidence of extensive cross slip in the Figure 2C were attributed to the presence of 0.4% nitrogen in the composition. The addition of N to a certain level can increase the stacking fault energy (Stoltz and Sande, 1980, Yonezawa et al. 2013, Kibey et al., 2006). Consequently, this leads to the reduction in the stacking faults and increases the chances for cross slip.

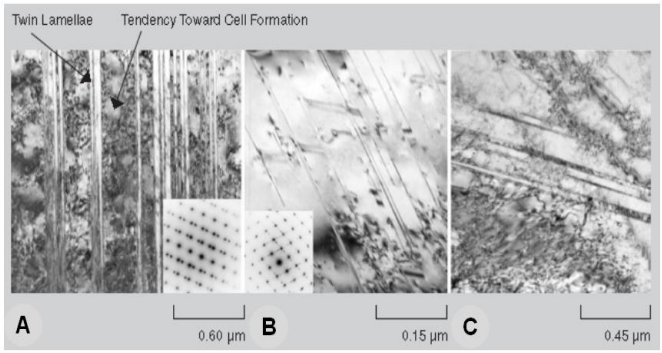

Figure 2: TEM Bright Field Images of ASS 316L Loaded in Tension along: [111] Direction to 15% Strain (A), [001] Direction to 10% Strain (B) and 0.4% N Alloyed Sample [011] Direction to 24% Strain (C) (Karaman et al., 2002).

IV. CONCLUSION

The following are the five conclusions at the end of the study investigating deformation twinning in cold rolled Austenitic Stainless Steels with Scanning Electron Microscopy and Electron Back Scatter Diffraction:

1. The study found evidence of deformation twin following cold rolling using Scanning Electron Microscopy and Electron Back Scatter diffraction techniques rather than Transmission Electron Microscopy.
2. It was suggested at the end of the study that the lattice distortion and the interaction of dislocation with twin boundaries within the grains are likely to cause increase in strength of material.
   The presence of relatively weak region caused by dislocation annihilation and hardened twin boundary region within the grain may facilitate strain heterogeneity and development of internal stresses.
4. The alternation of weak and hard region within the grains can influence transgranular propagation of crack in a susceptible environment.
5. It is therefore recommended that further characterisation of the cold rolled sample with Transmission Electron Microscopy could be carried out for in-depth analysis of the deformation substructures. This technique will enable access to the interaction of dislocations with twin bands.

V. ACKNOWLEDGEMENTS

The authors wish to thank Serco Assurance for their technical support. The technical supports from Professor Pete S. Bate and Mr David Strong during cold rolling at the Materials Science Centre, Manchester are duly acknowledged.

REFERENCES

Ahmed, I. I., Da Fonseca, J. Q. & Sherry, A. H. (2013). Effect of strain paths and residual delta ferrite on the failure of cold rolled austenitic stainless steels, type 304L. The Journal of Strain Analysis for Engineering Design, 48(7): 410-419.

Andresen, P. L., Morra, M. M. & Emigh, P. W. (2005). Effects of PWR primary water chemistry and deaerated water on SCC. Corrosion 2005.

Arioka, K., Yamada, T., Terachi, T. & Chiba, G. (2007). Cold work and temperature dependence of stress corrosion crack growth of austenitic stainless steels in hydrogenated and oxygenated high-temperature water. Corrosion, 63(12): 1114-1123.

ASM Handbook (2000). Properties and selection: irons, steels, and high performance alloys. ASM international.

Busby, J. & Was, G. (2005). Effect of metallurgical condition on irradiation-assisted stress corrosion cracking of commercial stainless steels. 12th International Conference on Environmental Degradation of Materials in Nuclear Power Systems-Water Reactors. Salt Lake City: The Minerals, Metals & Materials Society. 234-245.

Callister, W. D. (2003). Materials science and engineering: an introduction. John Wiley and Sons, New York.

Couvant, T., Legras, L., Vaillant, F., Boursier, J. & Rouillon, Y. (2005). Effect of strainhardening on stress corrosion cracking of AISI 304L stainless steel in PWR primary environment at 360 C. Proceedings of the 12th international conference on environmental degradation of materials in nuclear power system water reactors, TMS (The minerals, metals & materials society). 14-18.

Dieter, G. E. & Bacon, D. (1986). Mechanical metallurgy, McGraw-Hill, New York.

Elgun, S. Z. (1999). Plastic deformation. Available: http://info.lu.farmingdale.edu/depts/met/met205/plasticdeformation.html [Accessed 19/11/2010].

Enami, K. (2005). The effects of compressive and tensile prestrain on ductile fracture initiation in steels. Engineering fracture mechanics, 72(7): 1089-1105.

Fu, Y., Wu, X., Han, E.-H., Ke, W., Yang, K. & Jiang, Z. (2009). Effects of cold work and sensitization treatment on the corrosion resistance of high nitrogen stainless steel in chloride solutions. Electrochimica Acta, 54(5): 1618-1629.

Garcia, C., Martin, F., De Tiedra, P., Heredero, J. A. & Aparicio, M. L. (2000). Effect of prior cold work on intergranular and transgranular corrosion in type 304 stainless steels: quantitative discrimination by image analysis. Corrosion, 56(3): 243-255.

Garcia, C., Martin, F., Tiedra, P. D., Alonso, S. & M. L. Aparicio (2002). Stress corrosion cracking behaviour of cold-worked and sensitized type 304 stainless steels using the slow strain rate test. Corrosion, 58 (10): 849-857.

Garda, C. (2000). Effect of prior cold work on intergranular and transgranular corrosion in type 304 stainless steels: quantitative discrimination by image analysis. Corrosion, 56: 243.

Hagiwara, N., Masuda, T. & Oguchi, N. (2001). Effects of prestrain on fracture toughness and fatigue-crack growth of line pipe steels. Journal of Pressure Vessel Technology, 123(3): 355-361.

Jimenez, J. A. & Frommeyer, G. (2010). Analysis of the microstructure evolution during tensile testing at room temperature of high-manganese austenitic steel. Materials Characterization, 61(2): 221-226.

Kain, V., Chandra, K., Adhe, K. & De, P. (2004). Effect of cold work on low-temperature sensitization behaviour of austenitic stainless steels. Journal of Nuclear Materials, 334(2): 115-132.

Karaman, I., Sehitoglu, H., Chumlyakov, Y. & Maier, H. (2002). The deformation of low-stacking-fault-energy austenitic steels. JOM, 54(7): 31-37.

Kibey, S., Liu, J. B., Curtis, M. J., Johnson, D. D. & Sehitoglu, H. (2006). Effect of nitrogen on generalized stacking fault energy and stacking fault widths in high nitrogen steels. Acta Materialia, 54(11): 2991-3001.

Lee, T.-H., Oh, C.-S., Kim, S.-J. & Takaki, S. (2007). Deformation twinning in high-nitrogen austenitic stainless steel. Acta materialia, 55(11): 3649-3662.

Lozano-Perez, S., Yamada, T., Terachi, T., Schröder, M., English, C., Smith, G., Grovenor, C. & Eyre, B. (2009). Multi-scale characterization of stress corrosion cracking of cold-worked stainless steels and the influence of Cr content. Acta Materialia, 57(18): 5361-5381.

Murugesan, S., Kuppusami, P., Mohandas, E. & Vijayalakshmi, M. (2012). X-ray diffraction Rietveld analysis of cold worked austenitic stainless steel. Materials Letters, 67(1): 173-176.

Randle, V. & Engler, O. (2000). Introduction to texture analysis, macrotexture, microtexture and orientation mapping, Gordon and Breach Publishers.

Scheriau, S., Zhang, Z., Kleber, S. & Pippan, R. (2011). Deformation mechanisms of a modified 316L austenitic steel subjected to high pressure torsion. Materials Science and Engineering: A, 528(6): 2776-2786.

Spencer, K., Conlon, K., Brechet, Y. & Embury, J. (2009). The strain induced martensite transformation in austenitic stainless steels: Part 2 Effect of internal stresses on mechanical response. Materials Science and Technology, 25(1): 18-28.

Stoltz, R. E. & Sande, J. B. (1980). The effect of nitrogen on stacking fault energy of Fe-Ni-Cr-Mn steels. Metallurgical Transactions A, 11(6): 1033-1037.

Tsakiris, V. & Edmonds, D. (1999). Martensite and deformation twinning in austenitic steels. Materials Science and Engineering: A, 273: 430-436.

Wilkinson, A. J. & Britton, B. T. (2012). Strains, Planes, and EBSD in materials science. Materialstoday, 15(9): 366.

Yonezawa, T., Suzuki, K., Ooki, S. & Hashimoto, A. (2013). The effect of chemical composition and heat treatment conditions on stacking fault energy for Fe-Cr-Ni austenitic stainless steel. Metallurgical and Materials Transactions A, 44(13): 5884-5896.